

IceCube: the Discovery of High-Energy Cosmic Neutrinos

Francis Halzen^{*†}

University of Wisconsin–Madison, Madison, WI

E-mail: halzen@icecube.wisc.edu

We review the rationale for building kilometer-scale neutrino detectors and briefly describe the first such instrument, IceCube. It has transformed one cubic kilometer of natural Antarctic ice into a Cherenkov detector that maps the light patterns radiated by the secondary particles produced in neutrino interactions. We discuss the discovery of cosmic neutrinos and reappraise the properties of the flux after the recent doubling of the data from two to four years. We conclude that the flux is isotropic with a flavor composition of 1:1:1 and therefore most likely extragalactic in origin. It is large by any measure and consistent with a neutrino flux from sources that release a similar amount of energy in photons and, possibly, cosmic rays. Strikingly, the photon flux accompanying IceCube neutrinos is, after cascading through the extragalactic background light, consistent with the high-energy gamma-ray flux observed by Fermi. This observation suggests common sources, which should ease the task of identifying the cosmic accelerators producing IceCube neutrinos. We will argue that event rates of hundreds rather than tens per year are desirable for launching a new era of astronomy. Building a detector that instruments ten cubic kilometers of ice is realistic and, as a result of the large absorption length of the ice revealed by IceCube, comparable in scope to the original project.

XVI International Workshop on Neutrino Telescopes,

2-6 March 2015

Palazzo Franchetti, Istituto Veneto, Venice, Italy

^{*}Speaker.

[†]Discussion with collaborators inside and outside the IceCube Collaboration, too many to be listed, have greatly shaped this presentation. Thanks. This research was supported in part by the U.S. National Science Foundation under Grants No. ANT-0937462 and PHY-1306958 and by the University of Wisconsin Research Committee with funds granted by the Wisconsin Alumni Research Foundation.

1. The Status of Neutrino Astronomy

Astrophysical neutrinos unambiguously trace protons and nuclei throughout the Universe. The discovery of high-energy extraterrestrial neutrinos by IceCube with a flux at the very high level of those expected from cosmic ray accelerators brightens the prospect for identifying the sources [1]. The original observations specialized to neutrinos originating inside the detector, mostly showers initiated by electron and tau neutrinos. Since then, the conventional method of selecting upgoing muon tracks has delivered a sample of muon neutrinos with similar statistics but superior angular reconstruction [2]. Though limited to muon flavor, this analysis represents a watershed towards the identification of the sources. It has revealed secondary muon tracks that deposit several-hundred-TeV energy inside the detector, indicating PeV-energy parent neutrinos.

While the original data suggested the possibility of clustering near the Galactic center and the Galactic plane, the statistical evidence was not compelling and has not increased after doubling the number of events [3, 4, 5]. The observed neutrino flux is consistent with an isotropic distribution of arrival directions and equal contributions of all neutrino flavors [6] suggesting the observation of extragalactic sources whose flux has equilibrated in the three flavors after propagation over cosmic distances [7, 8]. Increasingly, a variety of analyses [6, 9] suggest that the cosmic neutrino flux dominates the atmospheric background above an energy that may be as low as 30 TeV with a spectrum that might not be described as a single power. This is reinforced by the fact that fitting the excess flux in different ranges of energy yields different values for the spectral index.

The most energetic neutrinos detected so far, with energies in the PeV range, should be produced by cosmic ray nucleons with an energy of 10-100 PeV. This corresponds to a source population contributing to the cosmic-ray spectrum between the “knee” and “ankle”; the latter has been traditionally associated with the transition from Galactic to extragalactic cosmic rays. Consequently, speculations on Galactic sources, like hypernovae or the Fermi bubbles, persist despite the accumulating evidence that IceCube is observing an isotropic flux of extragalactic sources. Candidate sources include active galactic nuclei or starburst galaxies. A source spectrum with a canonical E^{-2} shape is expected to produce several events with energies exceeding 2 PeV, including some at the Glashow resonance. None were observed, suggesting a break or cutoff. This spectral feature, if confirmed, can provide additional hints about the underlying source population.

The production of PeV neutrinos is inevitably associated with the production of PeV gamma rays. Hadronic accelerators produce fluxes of neutral and charged pions that are the parents of gamma rays and neutrinos, respectively. Gamma rays are attenuated over cosmic distances through the tenuous matter and radiation backgrounds of the Universe. They are predominantly absorbed by pair production in interactions with cosmic microwave and infrared background photons. With their absorption length roughly equal to the distance to the center of the Galaxy, the detection of PeV gamma rays would be a smoking-gun signal for Galactic sources; they have not been observed. In the case of extragalactic sources, however, the PeV gamma rays accompanying PeV neutrinos cascade down in energy to a diffuse gamma-ray flux in the GeV-TeV energy range. It is intriguing that this flux provides an excellent match to the extragalactic gamma-ray flux observed by the Fermi satellite; see Fig. 1 [10]. The matching relative magnitudes of the diffuse extragalactic gamma-ray flux detected by Fermi and the high-energy neutrino flux measured by IceCube suggest that they originated in common sources. This implies that most, possibly all, of the energy in the

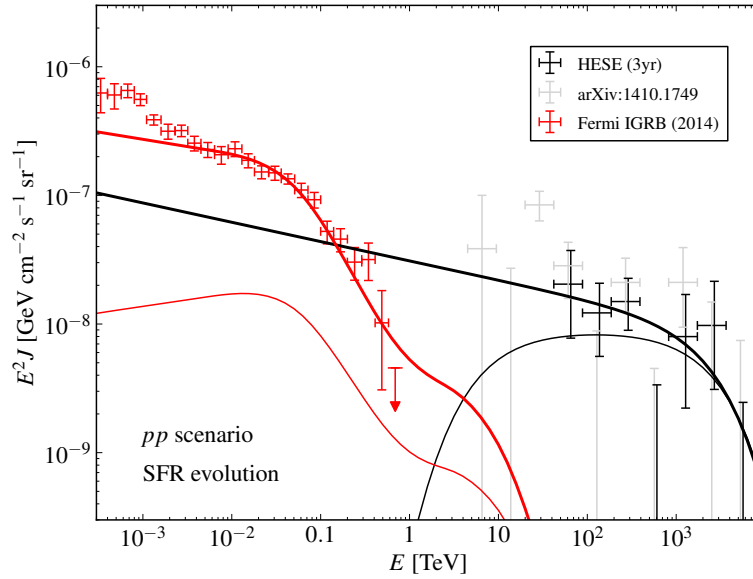


Figure 1: Two models of the astrophysical neutrino flux (black lines) observed by IceCube and the corresponding cascaded gamma-ray flux (red lines) observed by *Fermi*. The models assume that the decay products of neutral and charged pions from pp interactions are responsible for the non-thermal emission in the Universe [11]. The thin lines represent an attempt to minimize the contribution of the pionic gamma-ray flux to the Fermi observations. It assumes an injected flux of E^{-2} with exponential cutoff at low and high energy. The black data points are measured by the IceCube three-year “High-Energy Starting Event” (“HESE”) analysis [3], the gray data points are from an IceCube analysis lowering the energy threshold for events starting in the detector even further [9].

non-thermal universe originates in hadronic accelerators. Is it possible to escape this admittedly unexpected conclusion? In Fig. 1 we show an alternative match to the IceCube neutrino flux using a spectral shape more characteristic of neutrinos produced on a photon target by a beam of protons with a relatively flat spectrum. This provides a very poor description of the spectrum, which underestimates the neutrino flux yet requires a contribution to the Fermi photon spectrum above a level of 10%.

Interestingly, the observed neutrino flux saturates the Waxman-Bahcall bound [12] for neutrino emission from the sources of ultra-high-energy cosmic rays, which can be a natural consequence of cosmic ray “calorimetry,” or emission from cosmic-ray beam dumps generating roughly equal energies into photons and neutrinos and cosmic rays.

Later in this paper, we will elaborate on methods, including multiwavelength observations, to identify the sources and build on the discovery of cosmic neutrinos to launch a new astronomy. This will naturally suggest the concept of a next-generation detector, one that will instrument a volume ten times that of IceCube.

2. IceCube: the First Kilometer-Scale Neutrino Detector

Soon after the 1956 observation of the neutrino [13], the idea emerged that it represented the

ideal astronomical messenger [14, 15, 16]. The concept has since been demonstrated: neutrino detectors have “seen” the Sun and detected a supernova in the Large Magellanic Cloud in 1987. Both observations were of tremendous importance; the former showed that neutrinos have a tiny mass, opening the first chink in the armor of the Standard Model of particle physics, and the latter confirmed the basic nuclear physics of the death of stars.

High-energy neutrinos have a distinct potential to probe the extreme Universe. Neutrinos reach us from the edge of the Universe without absorption and with no deflection by magnetic fields. They can escape unscathed from the inner neighborhood of black holes and from the accelerators where cosmic rays are born. Their weak interactions also make neutrinos very difficult to detect. Immense particle detectors are required to collect cosmic neutrinos in statistically significant numbers [17, 18, 19, 20, 21, 22]. Already by the 1970s, it had been understood [23] that a kilometer-scale detector was needed to observe the “Greisen-Zatsepin-Kuzmin” GZK neutrinos produced in the interactions of cosmic rays with background microwave photons [24].

Above a threshold of $\sim 4 \times 10^{19}$ eV, cosmic rays interact with the microwave background introducing an absorption feature in the cosmic-ray flux, the Greisen-Zatsepin-Kuzmin (GZK) cut-off [25, 26]. The mean free path of extragalactic cosmic rays propagating in the microwave background is limited to less than 100 megaparsec. Therefore, secondary neutrinos produced in these interactions are the only probe of the still enigmatic sources at further distances. Realistic calculations [27, 28, 29] of the neutrino flux associated with the observed flux of extragalactic cosmic rays appeared in the 1970s and predicted on the order of one event per year in a kilometer-scale detector, subject to astrophysical uncertainties (for more recent updates see [30] and references therein). Today’s estimates of the sensitivity for observing potential cosmic accelerators such as Galactic supernova remnants, active galactic nuclei (AGN), and gamma-ray bursts (GRBs) unfortunately point to the same extreme requirement [17, 18, 19, 31, 21]. Building a neutrino telescope has been a daunting technical challenge.

Given the detector’s required size, early efforts concentrated on instrumenting large volumes of natural water with photomultipliers that detect the Cherenkov light emitted by the secondary particles produced when neutrinos interact with nuclei inside or near the detector [32, 33]. After a two-decade-long effort, building the Deep Underwater Muon and Neutrino Detector (DUMAND) in the sea off the main island of Hawaii unfortunately failed [34]. However, DUMAND pioneered many of the detector technologies in use today and inspired the deployment of a smaller instrument in Lake Baikal [35] as well as efforts to commission neutrino telescopes in the Mediterranean [36, 37, 38]. These have paved the way toward the planned construction of KM3NeT [39].

The first telescope on the scale envisaged by the DUMAND collaboration was realized instead by transforming a large volume of deep Antarctic ice into a particle detector, the Antarctic Muon and Neutrino Detector Array (AMANDA). In operation from 2000 to 2009, it represented the proof of concept for the kilometer-scale neutrino observatory, IceCube [40, 41], completed in 2010.

The IceCube neutrino detector (Fig. 2) consists of 86 strings, each instrumented with 60 ten-inch photomultipliers spaced 17 m apart over a total length of one kilometer. The deepest modules are located at a depth of 2.45 km so that the instrument is shielded from the large background of cosmic rays at the surface by approximately 1.5 km of ice. Strings are arranged at apexes of equilateral triangles that are 125 m on a side. The instrumented detector volume is a cubic kilometer of dark and highly transparent [42] Antarctic ice.

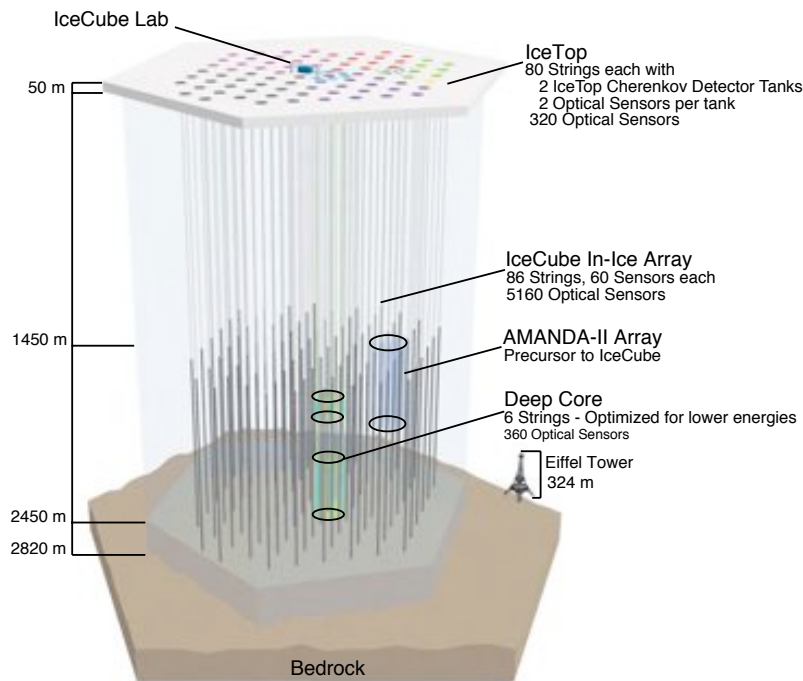


Figure 2: Sketch of the IceCube observatory.

Each digital optical module (DOM) consists of a glass sphere containing the photomultiplier and the electronics board that digitizes the signals locally using an onboard computer. The digitized signals are given a global time stamp with residuals accurate to less than 3 ns and are subsequently transmitted to the surface. Processors at the surface continuously collect the time-stamped signals from the optical modules, each of which functions independently. The digital messages are sent to a string processor and a global event builder. They are subsequently sorted into the Cherenkov patterns emitted by secondary muon tracks, or electron and tau showers, that reveal the direction and energy of the parent neutrino [43].

The depth of the detector and its projected area determine the trigger rate of approximately 3 kHz for penetrating muons produced by interactions of cosmic rays in the atmosphere above. The ratio of neutrino-induced signal to atmospheric background is on the order of one per million at TeV energy. The neutrino rate is dominated by neutrinos produced in the Earth's atmosphere. The first challenge is to select a sufficiently pure sample of neutrinos, and the second is to identify the small fraction that are astrophysical in origin.

Neutrino events may be broadly classified in two groups, muon tracks and particle showers (cascades), which reflect the patterns of Cherenkov light emitted by the charged particles produced when the neutrinos interact. Tracks are produced by charged current interactions of muon neutrinos while cascades are produced by charged current interactions of electron and tau neutrinos as well as neutral current interactions of all flavors. The travel range for ν_μ -induced muons is on the order of kilometers, while the length scale characteristic of the electromagnetic showers that dominate the cascade events is only tens of meters. Another way to classify neutrino events is to distinguish events that start inside the detector from those in which the neutrino interacts outside the detector.

The largest neutrino sample consists of ν_μ -induced muons entering the detector from zenith angles too large to be atmospheric in origin, typically $\theta \geq 85^\circ$. The rate of such events in the full IceCube detector is approximately 200 per day or more, depending on how the threshold for a particular analysis is set. The mean energy of this sample, dominated by atmospheric neutrinos, is $1 \sim 10$ TeV.

By specializing to events starting inside the detector, one instead observes neutrinos of all flavors. For $E_\nu < 1$ PeV the interaction of a ν_τ in IceCube will look much like that of a ν_e because the track length of the ν_τ of less than 50 m is smaller than the 125 m string spacings and difficult to identify. Analysis techniques are under development to remedy this.

Reconstruction of events depends on accurate timing (< 3 ns) and on the ability to measure the amount of Cherenkov light generated along the tracks of charged particles produced by the neutrino interactions. Basically, the arrival time of photons at the DOMs determines the trajectory and the amount of light determines the deposited energy. The number of photons produced per unit of path length and their distribution in wavelength are well-known quantities [44]. A detailed understanding of the properties of the propagation of the photons in the ice [42] is crucial to relate light generated to light observed in the DOMs. Reconstruction of tracks in ice has been well studied [45]. For typical kilometer tracks, the angular resolution is better than 0.4° . Reconstruction of cascade events is a topic of current study in IceCube [46]. Determining the deposited energy from the observed light pool is relatively straightforward, and a resolution of better than 15% is possible; the same value holds for the reconstruction of the energy deposited by a muon track inside the detector. The angular resolution for cascades is significantly poorer than for tracks. In the large cascades studied by detailed simulations on an event-by-event basis, it is possible to determine the directions to within 15° based on shapes of the photon timing patterns in each DOM, which reflect the directionality of the cascade electrons. At this point, IceCube's precision in shower reconstruction is limited by computing, not by the properties of the Cherenkov medium, guaranteeing improved performance in the future.

Atmospheric neutrinos are a background for cosmic neutrinos, at least at energies below ~ 100 TeV. Above this energy, their flux is too small to produce events in a kilometer-scale detector and every event is a discovery. This is how IceCube made its initial observation of cosmic neutrinos.

3. The Rationale for Building IceCube

Despite their discovery potential touching a wide range of scientific issues, from the search for dark matter to the study of neutrinos themselves, the construction of kilometer-scale neutrino detectors has been largely motivated by the prospect of detecting neutrinos associated with cosmic ray sources. Cosmic accelerators produce particles with energies in excess of 100 EeV; we still do not know where or how [47, 48, 49]. The bulk of the cosmic rays are Galactic in origin. Any association with our Galaxy presumably disappears at EeV energy when the gyroradius of a proton in the Galactic magnetic field exceeds its size. The cosmic-ray spectrum exhibits a rich structure above an energy of ~ 0.1 EeV, but where exactly the transition to extragalactic cosmic rays occurs is a matter of debate.

The detailed blueprint for a cosmic-ray accelerator must meet two challenges: the highest-energy particles in the beam must reach beyond 10^3 TeV (10^8 TeV) for Galactic (extragalactic)

sources, and their luminosities must be able to accommodate the observed flux. Both requirements represent severe constraints that have guided theoretical speculations.

Supernova remnants (SNRs) were proposed as a likely source of cosmic rays as early as 1934 by Baade and Zwicky [50]. It is interesting to note that they assumed the sources were extragalactic since the most recent observed supernova in the Milky way was in 1604. After diffusion in the interstellar medium was understood, supernova explosions in the Milky Way became the source of choice for the origin of Galactic cosmic rays [51], although after 50 years the issue is still debated [52]. The idea is widely accepted because of energetics. Three Galactic supernova explosions per century converting a reasonable fraction of a solar mass into particle acceleration can accommodate the steady flux of cosmic rays in the Galaxy.

Energetics also guides speculations on the origin of extragalactic cosmic rays. By integrating the cosmic-ray spectrum above the ankle at ~ 4 EeV, it is possible to estimate the energy density in extragalactic cosmic rays as $\sim 3 \times 10^{-19}$ erg cm $^{-3}$ [53]. This value is rather uncertain because of our ignorance of the precise energy where the transition from Galactic to extragalactic sources occurs. The power required for a population of sources to generate this energy density over the Hubble time of 10^{10} years is 2×10^{37} erg s $^{-1}$ per Mpc 3 . A gamma-ray-burst fireball converts a fraction of a solar mass into the acceleration of electrons, seen as synchrotron photons. The observed energy in extragalactic cosmic rays can be accommodated with the reasonable assumption that shocks in the expanding GRB fireball convert roughly equal energy into the acceleration of electrons and cosmic rays [54]. It so happens that 2×10^{51} erg per GRB will yield the observed energy density in cosmic rays after 10^{10} years, given that their rate is on the order of 300 per Gpc 3 per year. Hundreds of bursts per year over a Hubble time produce the observed cosmic-ray density, just as three supernovae per century accommodate the steady flux in the Galaxy.

Problem solved? Not really: it turns out that the same result can be achieved assuming that active galactic nuclei convert, on average, 2×10^{44} erg s $^{-1}$ each into particle acceleration [20]. As is the case for GRBs, this is an amount that matches their output in electromagnetic radiation. Whether GRBs or AGN, the observation that cosmic-ray accelerators radiate similar energies in photons and cosmic rays may not be an accident.

Neutrinos will be produced at some level in association with the cosmic-ray beam. Cosmic rays accelerated in regions of high magnetic fields near black holes or neutron stars inevitably interact with radiation surrounding them. Thus, cosmic-ray accelerators are beam dumps. Cosmic rays accelerated in supernova shocks interact with gas in the Galactic disk, producing equal numbers of pions of all three charges that decay into pionic photons and neutrinos. A larger source of secondaries is likely to be gas near the sources, for example cosmic rays interacting with high-density molecular clouds that are ubiquitous in the star-forming regions where supernovae are more likely to explode. For extragalactic sources, the neutrino-producing target may be electromagnetic, for instance, photons radiated by the accretion disk of an AGN or synchrotron photons that coexist with protons in the expanding fireball producing a GRB. In Fig. 3, estimates of astrophysical neutrino fluxes are compared with measurements of atmospheric neutrinos. The shaded band indicates the level of model-dependent expectations for high-energy neutrinos of astrophysical origin. The estimates, discussed briefly in the next paragraphs, set the level at

$$E_\nu^2 dN_\nu/dE_\nu \simeq 10^{-8} \text{ GeV cm}^{-2} \text{ s}^{-1} \text{ sr}^{-1} \quad (3.1)$$

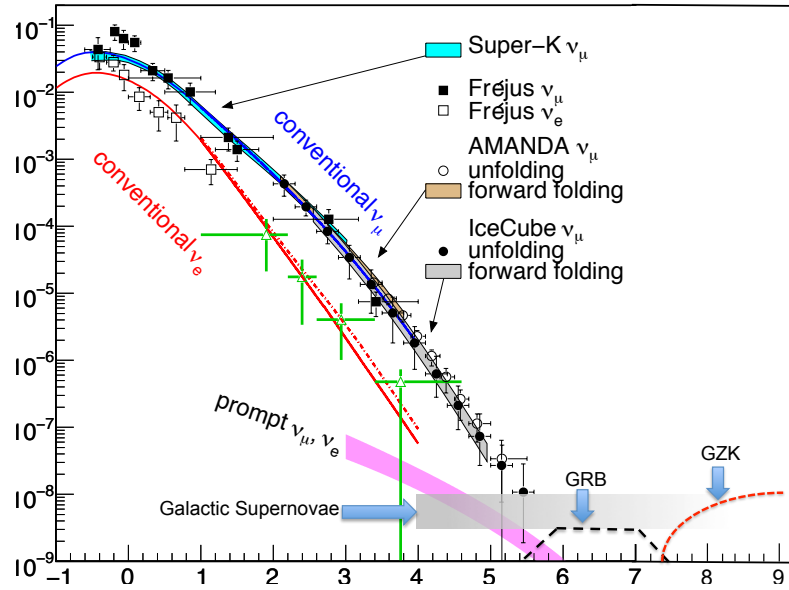


Figure 3: Anticipated astrophysical neutrino fluxes produced by supernova remnants and GRBs exceed the atmospheric neutrino flux in IceCube above 100 TeV because of their relatively hard E^{-2} spectrum. Also shown is a sample calculation of the GZK neutrino flux. The atmospheric electron-neutrino spectrum (green open triangles) is from [42]. The conventional ν_e (red line) and ν_μ (blue line) from Honda, ν_e (red dotted line) from Bartol and charm-induced neutrinos (magenta band) [55] are shown. Previous measurements from Super-K [56], Frejus [57], AMANDA [58, 59] and IceCube [60, 61] are also shown. Details about the theoretical estimates shown can be found in Ref. [43].

per flavor, or somewhat less.

Estimating the neutrino flux associated with cosmic rays accelerated in SNRs and GRBs is relatively straightforward as both the beam, identified with the observed cosmic-ray flux, and the targets, observed by astronomers, are known. In the case of SNRs, the main uncertainty is the availability of nearby target material. In the case of GRBs, the main uncertainty is the fraction of the extragalactic cosmic ray population that comes from this source.

Active galaxies are complex systems with many possible sites for accelerating cosmic rays and for targets to produce neutrinos. For example, if acceleration occurs mainly at an outer termination shock in intergalactic space [62], there would be little target material available. One generic picture in which the neutrino luminosity is directly related to the contribution of the sources to extragalactic cosmic rays arises if acceleration occurs in the jets of AGN (or GRBs) [63, 64]. High-energy protons interact in the intense radiation fields inside the jets. In the $p\gamma \rightarrow p\pi^0$ channel, the protons remain in the accelerator. In the $p\gamma \rightarrow n\pi^+$ channel, however, the neutrons escape and eventually decay to produce cosmic-ray protons, while the pions decay to neutrinos. The luminosity of neutrinos from photo-pion production is then directly related by kinematics to the cosmic-ray protons that come from decay of the escaping neutrons.

TeV gamma rays are measured from many AGN blazars [65]. Although the observed gamma rays are likely to be from accelerated electrons, which radiate more efficiently than protons, the

gamma-ray luminosity may give an indication of the overall cosmic-ray luminosity and hence of the possible level of neutrino production [66]. In this context, we introduce Fig. 4 [67] showing IceCube upper limits [68] on the neutrino flux from nearby AGN as a function of their distance. The sources at red shifts between 0.03 and 0.2 are Northern Hemisphere blazars for which distances and intensities are listed in TeVCat [65] and for which IceCube also has upper limits. In several cases, the muon-neutrino limits have reached the level of the TeV photon flux. One can sum the sources shown in the figure into a diffuse flux. The result, after accounting for the distances and luminosities, is $3 \times 10^{-9} \text{ GeV cm}^{-2} \text{ s}^{-1} \text{ sr}^{-1}$, or approximately $10^{-8} \text{ GeV cm}^{-2} \text{ s}^{-1} \text{ sr}^{-1}$ for all neutrino flavors. This is only a factor of 3 below the generic astrophysical neutrino flux of Eq. 3.1. At this intensity, neutrinos from theorized cosmic-ray accelerators will cross the steeply falling atmospheric neutrino flux above an energy of $\sim 300 \text{ TeV}$; see Fig. 3. The level of events observed in a cubic-kilometer neutrino detector is 10–100 ν_μ -induced events per year. Such estimates reinforced the logic for building a cubic kilometer neutrino detector. A more detailed description of the theoretical estimates can be found in reference [43].

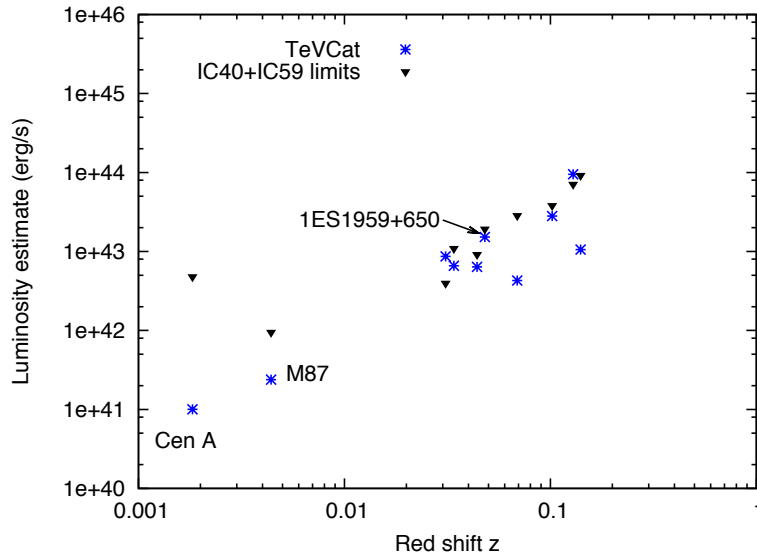


Figure 4: Limits on the neutrino flux from selected active galaxies derived from IceCube data taken during construction when the instrument was operating with 40 and 59 strings of the total 86 instrumented strings of DOMs [68]. These are compared with the TeV photon flux for nearby AGN. Note that energy units are in ergs, not TeV.

3.1 Discovery of Cosmic Neutrinos

The generation of underground neutrino detectors that preceded the construction of the AMANDA detector searched for cosmic neutrinos without success and established an upper limit on their flux, assuming an E^{-2} energy dependence [57]:

$$E_\nu^2 \frac{dN}{dE_\nu} \leq 5 \times 10^{-9} \text{ TeV cm}^{-2} \text{ s}^{-1} \text{ sr}^{-1} \quad (3.2)$$

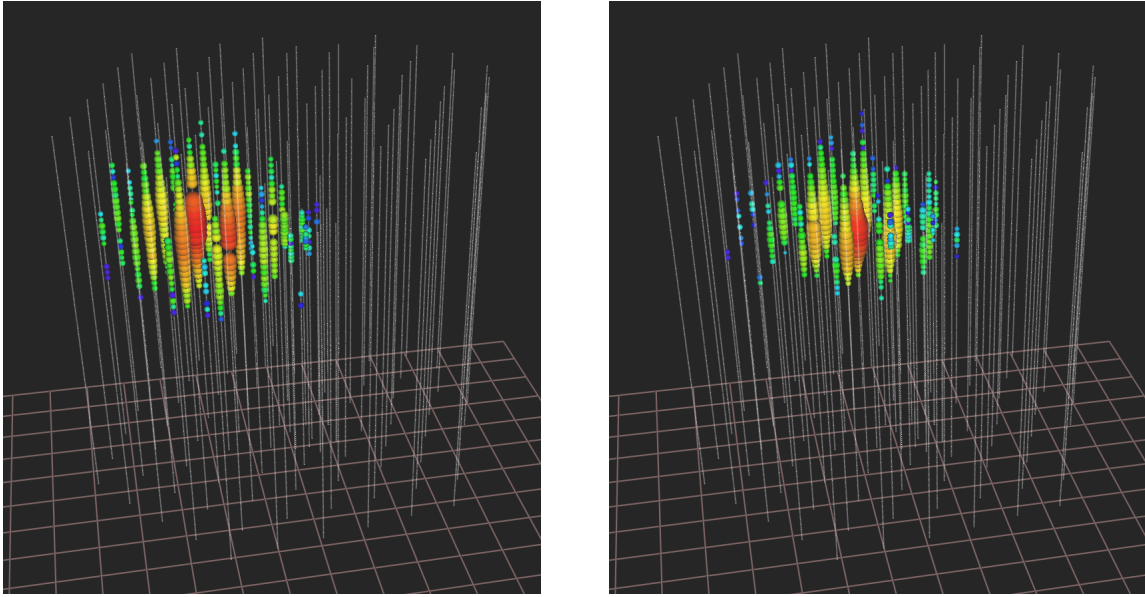


Figure 5: Light pool produced in IceCube by the two cascades “Bert” (left) and “Ernie” (right). The measured energy is 1.04 PeV and 1.14 PeV, respectively, which represents a lower limit on the energy of the neutrino that initiated the shower. The vertical lines of white dots represent the sensors that report any detected signal. Color of the dots indicates arrival time, from red (early) to purple (late) following the rainbow. Size of the dots indicates the number of photons detected.

Operating for almost one decade, the AMANDA detector improved this limit by two orders of magnitude. With data taken during its construction, IceCube’s sensitivity rapidly approached the theoretical flux estimates for candidate sources of cosmic rays such as supernova remnants, γ -ray bursts and, with a larger uncertainty, active galactic nuclei; see Fig. 3. With its completion, IceCube also positioned itself for observing the much anticipated flux of GZK neutrinos, with some estimates predicting as many as two events per year.

GZK neutrinos were the target of a dedicated search using IceCube data collected between May 2010 and May 2012. Two events were found [69]. However, their energies, rather than EeV, as expected for GZK neutrinos, were in the PeV range: 1,040 TeV and 1,140 TeV. The events are particle showers initiated by neutrinos interacting inside the instrumented detector volume. Their light pool of roughly one hundred thousand photoelectrons extends over more than 500 meters; see Fig. 5. With no evidence of a muon track, they are showers initiated by electron or tau neutrinos.

Previous to this serendipitous discovery, neutrino searches had almost exclusively specialized to the observation of muon neutrinos that interact primarily outside the detector to produce kilometer-long muon tracks passing through the instrumented volume. Although creating the opportunity to observe neutrinos interacting outside the detector, it is necessary to use the Earth as a filter to remove the huge background flux of muons produced by cosmic ray interactions in the atmosphere. This limits the neutrino view to a single flavor and half the sky. Inspired by the observation of the two PeV events, a filter was designed that exclusively identifies neutrinos interacting inside the detector. It divides the instrumented volume of ice into an outer veto shield and a 420 megaton inner fiducial volume. The separation between veto and signal regions was

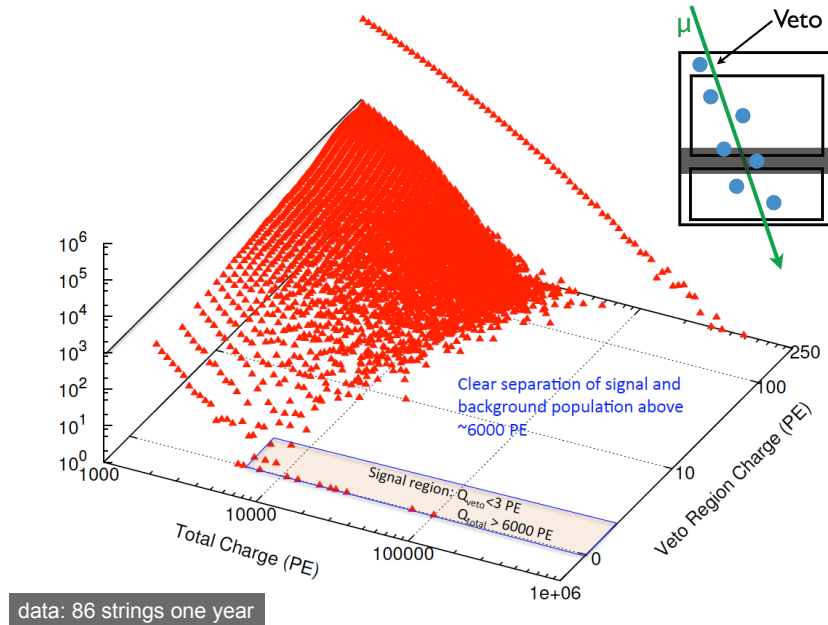


Figure 6: One year of IceCube data from its final 86-string configuration showing number of events as a function of the total number of photoelectrons and the number present in the veto region. The signal region requires more than 6000 photoelectrons with less than three of the first 250 in the veto region of the detector. The signal, including nine events with reconstructed neutrino energy in excess of 100 TeV, is clearly separated from the background.

optimized to reduce the background of atmospheric muons and neutrinos to a handful of events per year while keeping 98% of the signal. The great advantage of specializing to neutrinos interacting inside the instrumented volume of ice is that the detector functions as a total absorption calorimeter measuring energy with a 10–15% resolution. Also, neutrinos from all directions in the sky can be identified, including both muon tracks produced in ν_μ charged-current interactions and secondary showers produced by neutrinos of all flavors.

Analyzing the data covering the same time period as the GZK neutrino search, 28 candidate neutrino events were identified with in-detector deposited energies between 30 and 1140 TeV; see Fig. 6. Of these, 21 are showers whose energies are measured to better than 15% but whose directions are determined to 10–15 degrees only. Predominantly originating in the Southern Hemisphere, none show evidence for an accompanying muon track signaling the production of the neutrino in an atmospheric shower. If atmospheric in origin, the neutrinos should indeed be accompanied by muons produced in the air shower in which they originate. For guidance, at 1 PeV, less than 0.1% of atmospheric showers contain no muons with energy above 500 GeV, approximately that which is needed to reach the detector in the deep ice when traveling vertically.

The remaining seven events are muon tracks, which do allow for subdegree angular reconstruction; only a lower limit on their energy can be established because of the unknown fraction carried away by the exiting muon track. Furthermore, with the present statistics, these are difficult to separate from a remnant of the competing atmospheric muon background. The 28 events include

the two PeV events previously revealed in the GZK neutrino search.

Fitting the data to a superposition of extraterrestrial neutrinos on an atmospheric background yields a cosmic neutrino flux of

$$E_\nu^2 \frac{dN}{dE_\nu} = 3.6 \times 10^{-11} \text{ TeV cm}^{-2} \text{ s}^{-1} \text{ sr}^{-1} \quad (3.3)$$

for the sum of the three neutrino flavors. As discussed in the previous section, this is the level of flux anticipated for neutrinos accompanying the observed cosmic rays. Also, the energy and zenith angle dependence observed is consistent with what is expected for a flux of neutrinos produced by cosmic accelerators; see Figs. 7 and 8. The flavor composition of the flux is, after corrections for the acceptances of the detector to the different flavors, consistent with $\nu_e : \nu_\mu : \nu_\tau \sim 1 : 1 : 1$ as anticipated for a flux originating in cosmic sources.

Clearly, the major uncertainty in the spectrum of atmospheric neutrinos at high energy is the level of charm production that must be present at some level. The short-lived charmed hadrons preferentially decay up to a characteristic energy of 10^7 GeV, producing prompt muons and neutrinos with the same spectrum as their parent cosmic rays. This prompt flux of leptons has not yet been measured. Fits to both starting-event and upgoing muon-neutrino-data samples prefer a vanishing charm component. Existing limits [70, 71] allow a charm component at a level predicted by a dipole model calculation for the high-energy charm cross section [55]. In this context, it is important to point out that the muon produced in the same decay as the neutrino is guaranteed to reach the detector for muon neutrinos from above when the neutrino energy is sufficiently high and the zenith angle sufficiently small [72]. In this case, the atmospheric neutrino provides its own self-veto. This self-veto is routinely applied to the data sample and further suppresses any potential charm component.

Two additional years of data have been taken with the completed detector (2012-2014), and the analysis of the first of these has been published [3]. Applying an identical analysis to the four-year data yield results that are consistent with those described in the discovery paper. In combining the four years of data, a purely atmospheric explanation can be excluded at 7σ . The four-year data set contains a total of 54 neutrino events with deposited energies ranging from 30 to 2000 TeV. The 2000 TeV event is the highest energy neutrino interaction ever observed. Note that Figs. 7 and 8 show the four-year sample. In the fourth year, two muon neutrinos were found whose deposited energies inside the detector likely require PeV-energy parent neutrinos. One of them was reconstructed through IceTop with little evidence for an air shower. Combining the absence of an air shower in IceTop and of cosmic-ray muons in IceCube with the high energy results in a high significance for a single event to be of astrophysical origin.

Additionally, a totally independent analysis of the spectrum of muon neutrinos passing through the Earth has confirmed the existence of the astrophysical component first observed in neutrino events starting inside the detector. Because of their significantly harder energy spectrum, a flux of astrophysical neutrinos as observed in the starting-event analysis should populate, in fact dominate, the spectrum of muon-induced neutrinos beyond the steepening atmospheric flux. The spectrum of the atmospheric neutrino background becomes indeed one power steeper than the spectrum of primary cosmic rays at high energy as the competition between interaction and decay of pions and kaons increasingly suppresses their decay. A further steepening occurs above 100 TeV as a

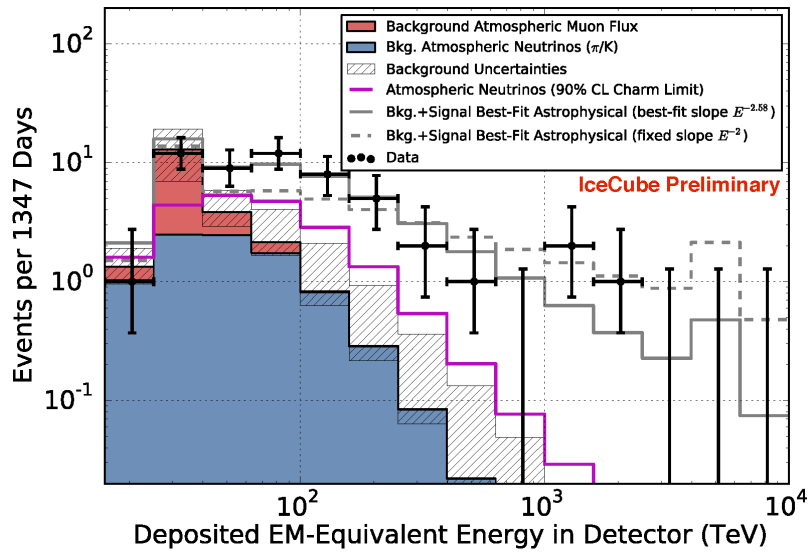


Figure 7: Deposited energies of events observed in four years of data with predictions. The hashed region shows uncertainties on the sum of all backgrounds. Muons (red) are computed from simulation to overcome statistical limitations in our background measurement and scaled to match the total measured background rate. Atmospheric neutrinos and uncertainties thereon are derived from previous measurements of both the π, K and charm components of the atmospheric spectrum [73].

consequence of a steepening in the primary spectrum, the so-called “knee.” As already discussed, atmospheric neutrino events with energies exceeding 100 TeV are therefore rare, on the order of one event per year even in a detector the size of IceCube.

An analysis of the same two years of data used for the starting-event analysis has revealed an excess of high-energy ν_μ -induced muons penetrating the Earth from the Northern Hemisphere [2]. Their spectrum is consistent with the one obtained in the starting event analysis; see Fig. 9. Shown is the muon neutrino flux as a function of the energy deposited by the muons inside the detector. This reflects the energy of the neutrino that initiated the events; for instance, the highest energies in Fig. 9 correspond, on average, to parent neutrinos of PeV energy. A best fit to the spectrum that includes a conventional, charm and astrophysical component with free normalizations yields the results shown in the figure.

Where do the cosmic neutrinos originate? Figure 10 shows the arrival directions of the four-year starting-event sample in Galactic coordinates in terms of cascade events (+) and track events (\times). The color scale indicate the value of the test statistic (TS) of an unbinned maximum likelihood test searching for anisotropies of the event arrival directions. No significant local excess in the sky was found when compared to randomized pseudo-experiments. The correlation with the Galactic plane is also not significant: when letting the width float freely, the best fit returned a value of 7.5° (indicated as horizontal red lines in Fig. 10) with a post-trial chance probability of 3.3%. The horizontal red lines in Fig. 10 indicate the minimum width and step-size of $\pm 2.5^\circ$ used in the scan. The high Galactic latitudes of some of the high-energy events suggest an extragalactic component at some level. Neither probability decreased with the doubling of the data. The IceCube Collaboration also searched for clustering of the events in time and investigated a possible correlation with the

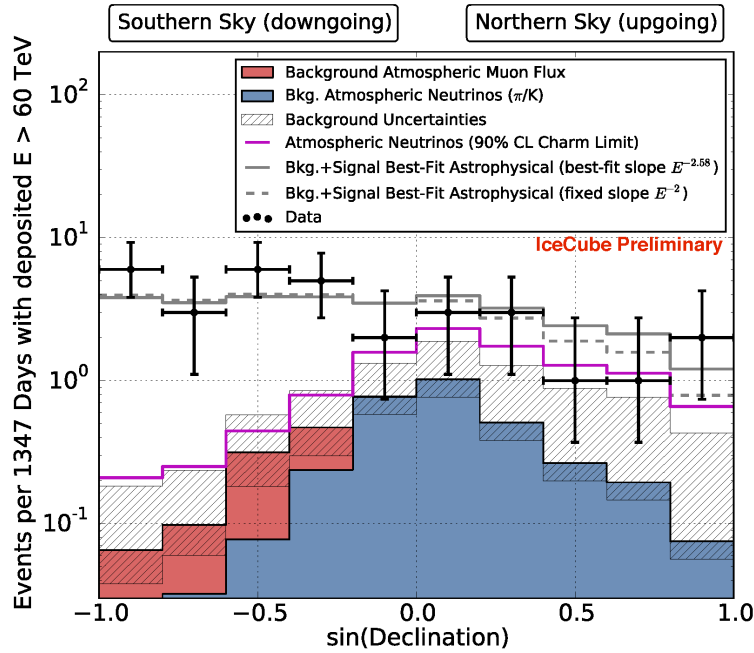


Figure 8: Arrival angles of events with $E_{dep} > 60$ TeV. The increasing opacity of the Earth to high-energy neutrinos suppresses the signal to the right of the plot. Vetoing atmospheric neutrinos by muons from their parent air showers depresses the atmospheric neutrino background on the left. The data are described well by an astrophysical isotropic E^{-2} spectrum assuming equal contributions of all three neutrino flavors.

times of observed GRBs. No statistically significant correlation was found.

The picture emerges that the cosmic neutrino flux observed is isotropic and therefore extragalactic in origin, consistent with the indication for a 1:1:1 flavor composition. A subdominant Galactic component cannot be excluded. Although the sources have not been identified, the key indication at this point is that the overall level of the flux is high, consistent with the assumption that IceCube and Fermi are to a large extent detecting the same extragalactic sources; see Fig. 1.

4. The Road Ahead

The absence of a strong anisotropy of neutrino arrival directions raises the possibility that the cosmic neutrinos originate from a number of relatively weak extragalactic sources. It is indeed important to keep in mind that the interaction rate of a neutrino is so low that it travels unattenuated over cosmic distances through the tenuous matter and radiation backgrounds of the Universe. This makes the identification of individual point sources contributing to the IceCube flux challenging [74, 75, 76, 77]. Even so, it is also important to realize that IceCube is capable of localizing the sources by observing multiple neutrinos originating in the same location. Not having observed neutrino clusters in the present data raises the question of how many events are required to make such a model-independent identification possible. The answer to this question suggests the construction of a next-generation detector that instruments a ten-times-larger volume of ice [10]. Interestingly, this can be achieved by only doubling the number of optical sensors of the present instrument. We will return to this last point later.

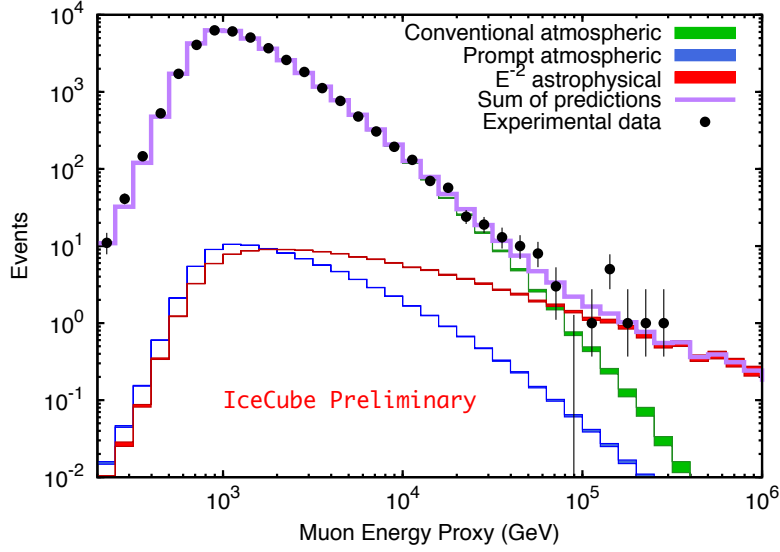


Figure 9: Spectrum of secondary muons initiated by muon neutrinos that have traversed the Earth, i.e., with zenith angle less than 5° above the horizon, as a function of the energy they deposit inside the detector. The highest energy muons are, on average, initiated by PeV neutrinos.

Following the analysis [77], let's estimate [77] the number of cosmic neutrinos required to detect a spatial cluster of m , or more, neutrino events from the same source. The observed cluster will most likely come from a nearby source and we can hence simplify the calculation by considering Euclidean space. The number of events $n(r)$ from a local source at a distance $r \leq H_0^{-1}$, i.e., smaller than the Hubble radius, is

$$n(r) \simeq \frac{H_0}{f_{\text{sky}} 4\pi r^2 \xi_z} \times \frac{N}{\rho_0} \quad (4.1)$$

Here N is the number of events from all sources with a local density ρ_0 and the cosmological evolution of the sources is parametrized by an effective parameter ξ_z . For instance, assuming that the cosmic ray sources track star formation, $\xi_z \simeq 2.4$. The local Hubble constant H_0 sets the effective size, c/H_0 , of the observable Universe (and in this way solves the neutrino variant of Olbers' paradox for infinite homogeneous neutrino source distributions). Finally, f_{sky} is the sky coverage of the detector in units of 4π .

As a back-of-the-envelope estimate of the required total number of events for the observation of event multiplets, we consider the contribution of the closest source expected in the field of view (FoV) within a sphere of volume $V_1 = 1/(f_{\text{sky}} \rho_0)$. The total number of events that we expect from this volume is given by the integral of Eq. (4.1) over V_1 and yields $m = N(V_1/V_H)^{1/3}/\xi_z$ where we introduce the Hubble volume $V_H = 4\pi/(3H_0^3)$. Note that V_H/V_1 corresponds to the effective number of sources in the FoV. In the case of continuous sources, we arrive then at an expected total for m local events of

$$N \simeq 740 \left(\frac{m}{2}\right) \xi_{z,2.4} (f_{\text{sky}} \rho_{0,-5})^{1/3}. \quad (4.2)$$

Therefore, to observe a cluster of events from the nearest source requires a sample of $\sim 1,000$ neutrinos for a local source density of $\rho_0 = 10^{-5} \text{Mpc}^{-3}$, the characteristic local density of AGNs. Other source candidates may have larger or smaller densities but notice that the dependence of

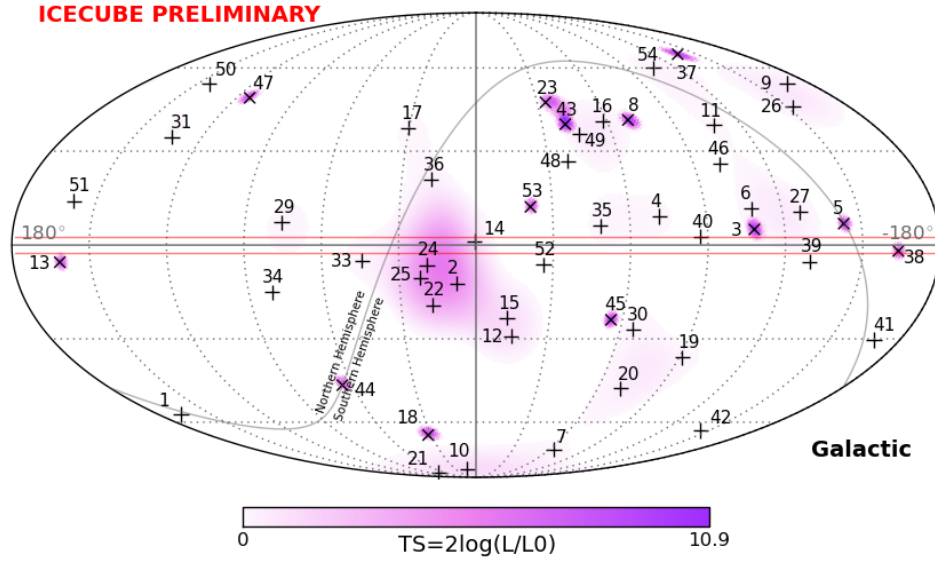


Figure 10: Sky map in Galactic coordinates of the test statistic (TS) that measures the probability of clustering among the 54 events from the four-year starting-event data sample [4]. Shower-like events are identified by a vertical cross (+), those containing muon tracks by an angled cross (×).

the number of events required on the density is relatively weak. Still, it will realistically require a sample of more than a thousand neutrino events with good angular resolution and little background to identify the sources. This would take roughly 20 years or so with the present instrument. An instrument with 5 – 10 times the sensitivity of IceCube is required to operate as an effective telescope collecting a thousand events in a few years. Detailed calculations that take into account ensemble variations of the source distribution as well as the event statistics of individual sources can be found in reference [77].

A higher signal-to-background ratio can be achieved if the observed events are variable in time, typical for extragalactic sources [77]. In the case of transient sources, we have to take into account that the number of sources is increasing with observation time $T_{\text{live}} = N/\dot{N}$. Solving in terms of the total observation rate \dot{N} we arrive at

$$N \simeq 637 \left(\frac{m}{2}\right)^{\frac{3}{2}} \xi_{z,2.4}^{\frac{3}{2}} (f_{\text{sky}} \dot{\rho}_{0,-6} / \dot{N}_2)^{\frac{1}{2}}, \quad (4.3)$$

with an event rate $\dot{N} = 100\dot{N}_2/\text{yr}$. In the case of rare transient sources like long duration GRBs with (isotropic equivalent) rate density of $\dot{\rho}_0 \simeq 10^{-9} \text{Mpc}^{-3} \text{yr}^{-1}$ [78], an identification of the sources with IceCube itself is still likely.

Significantly fewer events are required to identify the source population if the observed events can be correlated with astronomical catalogues [77]. In fact, a recent study looking for the combined neutrino emission of *Fermi* identified blazars [79] could place upper limits on their contribution to the IceCube observation at the level of a few 10%. A related population study has recently been carried out in Ref. [80]. Also, the contribution of GRBs to the diffuse emission is limited to

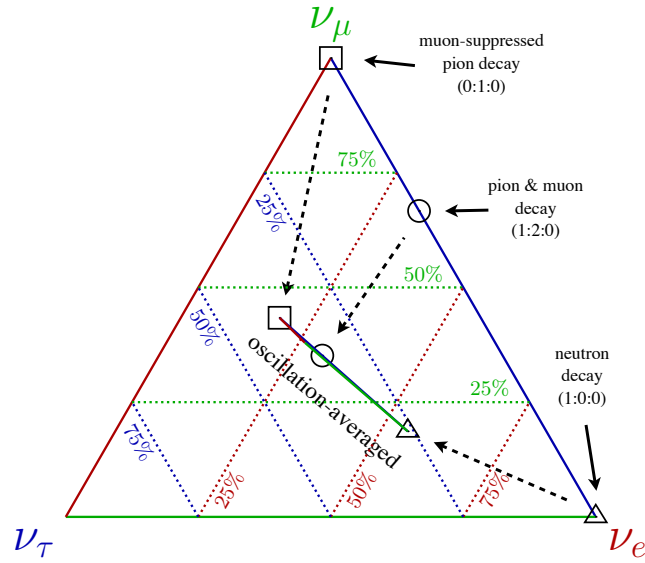


Figure 11: Neutrino flavor phase space after oscillation. We use the best-fit oscillation parameters $\sin^2 \theta_{12} = 0.304$, $\sin^2 \theta_{23} = 0.577$, $\sin^2 \theta_{13} = 0.0219$, and $\delta = 251^\circ$ following Ref. [83] updated after *Neutrino 2014* [84]. Each position in the triangle parametrizes a general initial flavor ratio ($\nu_e : \nu_\mu : \nu_\tau$). We also indicate specific ratios for neutron decay and pion production. The inner triangle is the corresponding observable phase space after decoherence of the neutrino flavor state over large times or distances.

less than 10% due to strong IceCube’s limit on the prompt neutrino emission of GRBs coincidence with the gamma-ray display [81].

Despite the degraded resolution and the reduced potential for astronomy, the observation of electron and tau neutrinos should still be a priority. They complement the sky coverage of up-going muon neutrinos that, at PeV energy, are mostly detected near the horizon because they are absorbed by the Earth. At high energies, neutrino production can happen in the production and decay of unstable nuclei, e.g., neutrons with $n \rightarrow pe^- \bar{\nu}_e$, or mesons, e.g., $\pi^+ \rightarrow \mu^+ \nu_\mu$. Note that the neutrino production from the decay of muons $\mu^+ \rightarrow e^+ \nu_e \bar{\nu}_\mu$ can be suppressed relative to the pion decay channel if synchrotron losses are important. Hence, the flavor composition is likely energy dependent and provides insight into the relative energy loss of high-energy pions and muons in the magnetic field of the cosmic accelerator [82].

Various authors have studied the implications of IceCube’s HESE (high-energy starting-event) topologies with astrophysical and/or exotic production mechanisms [85, 86, 87, 88, 89, 90, 91, 92]. Figure 11 shows the general neutrino flavor phase space $\nu_e : \nu_\mu : \nu_\tau$ and the expected intrinsic flavor ratio in astrophysical sources from neutron decay (triangle), pion+muon decay (circle), and muon-damped pion decay (square). The observable neutrino flavor ratio is expected to be averaged over many oscillations. This leaves only a very narrow flavor composition, which is shown as the flat triangle inset in the center of Fig. 11. The corresponding observable flavor ratios of the three astrophysical production mechanisms are also indicated. The final parameter space is very close to the “tri-bi-maximal” approximation of mixing angles, which predicts that the final flavor ratio depends only on the initial electron neutrino ratio $x = N_{\nu_e} / N_{\nu_{\text{tot}}}$ and $(2/3 + x) : (7/6 - x/2) : (7/6 -$

$x/2$).

The precise relation between HESE topologies and flavor composition is non-trivial, since atmospheric backgrounds and detector effects have to be taken into account properly. In a recent IceCube analysis [6] it was shown that the observation of tracks and cascades is consistent with most astrophysical scenarios within uncertainties. At sub-PeV energies (before ν_τ events can be distinguished from single cascades) the observation is mostly degenerate in terms of the total $\nu_e + \nu_\tau$ ratio, except for the contribution of prompt tau decays into muons. The expected fraction for tracks out of the total number events is about $7/24 - x/8$, where we take into account that CC interactions are about three times larger than neutral current interactions at these energies. The uncertainty of the inferred intrinsic electron-neutrino fraction x is hence about eight times higher than the uncertainty of the track fraction. The situation becomes even more challenging if we include backgrounds and systematic uncertainties.

The situation of flavor identification improves at super-PeV neutrino energies. On one hand, the decay length of the τ produced in CC ν_τ interactions becomes resolvable by the detector and can in principle be distinguished from tracks and cascade events as argued before. On the other hand, electron anti-neutrinos $\bar{\nu}_e$ can resonantly interact with in-ice electrons via the Glashow resonance, $\bar{\nu}_e e^- \rightarrow W^-$, at neutrino energies of about 6.3 PeV. This could be observable as a peak in the cascade spectrum, depending on the relative contribution of $\bar{\nu}_e$ after oscillation. In principle, this will allow us to answer the basic question of whether the cosmic neutrinos are photo- or hadro-produced in the source with different neutrino-to-anti-neutrino ratios [93, 94].

Construction of a next-generation instrument with at least five times higher sensitivity would likely result in the observation of GZK neutrinos [10]. The rate expected with IceCube currently is only one event per year, assuming that all cosmic rays are protons (and, it is difficult to imagine that not a significant component of the highest energy neutrinos would be protons). Obviously, higher sensitivity would also benefit the wide range of measurements performed with the present detector, from the search for dark matter to the precision limits on any violation of Lorentz invariance.

By building IceCube, it was possible to map the optical properties of natural ice over large distances, and the IceCube Collaboration made the surprising discovery that the absorption length of the Cherenkov light to which the DOMs are sensitive exceeds 100 m. In fact, in the lower half of the detector it exceeds 200 m. Although the optical properties vary with the layered structure of the ice, the average absorption length dictates the distance by which one can space the strings of sensors without spoiling the uniformity of the detector. Modeling indicates that spacings of 250 m, possibly larger, are acceptable. One can thus sufficiently instrument a ten-times-larger volume of ice with the same number of strings used to build IceCube. The project would be free of risk since the performance of the DOMs is understood and we know how to deploy them. Furthermore, the costs are understood. Designed before 1999, all of the components of IceCube can be significantly updated for improved performance.

The larger spacings do of course result in a higher threshold but this is not necessarily bad. While the 100,000 or so atmospheric neutrinos that IceCube collects above a threshold of 100 GeV every year were useful for calibration, they represent a severe background for isolating the cosmic component of the flux. The peak sensitivity to an E^{-2} spectrum is reached at 40 TeV [95]. While the detector has to be efficient below that energy, a threshold much lower than this value introduces background without a gain in signal. Designs for a next-generation instrument are in progress [10].

References

- [1] M. G. Aartsen *et al.* (IceCube) 2013 *Science* **342** 1242856 [[1311.5238](#)]
- [2] C. Weaver 2014 Spring APS Meeting, Savannah, Georgia, USA
- [3] M. Aartsen *et al.* (IceCube Collaboration) 2014 *Phys.Rev.Lett.* **113** 101101 [[1405.5303](#)]
- [4] O. Botner 2015 IPA Conference, IceCube, Wisconsin, USA
- [5] M. Ahlers, Y. Bai, V. Barger and R. Lu 2015 [[1505.03156](#)]
- [6] M. Aartsen *et al.* (IceCube Collaboration) 2015 [[1502.03376](#)]
- [7] J. G. Learned and S. Pakvasa 1995 *Astropart.Phys.* **3** 267–274 [[hep-ph/9405296](#)]
- [8] H. Athar, M. Jezabek and O. Yasuda 2000 *Phys.Rev.* **D62** 103007 [[hep-ph/0005104](#)]
- [9] M. Aartsen *et al.* (IceCube Collaboration) 2014 [[1410.1749](#)]
- [10] M. Aartsen *et al.* (IceCube Collaboration) 2014 [[1412.5106](#)]
- [11] K. Murase, M. Ahlers and B. C. Lacki 2013 *Phys.Rev.* **D88** 121301 [[1306.3417](#)]
- [12] E. Waxman and J. N. Bahcall 1999 *Phys.Rev.* **D59** 023002 [[hep-ph/9807282](#)]
- [13] F. Reines and C. L. Cowan 1956 *Nature* **178** 446–449
- [14] K. Greisen 1960 *Ann.Rev.Nucl.Part.Sci.* **10** 63–108
- [15] F. Reines 1960 *Ann.Rev.Nucl.Part.Sci.* **10** 1–26
- [16] M. Markov 1960 *Proc. of the 10th Intl. Conf. on High-Energy Physics* 578–581
- [17] T. K. Gaisser, F. Halzen and T. Stanev 1995 *Phys.Rept.* **258** 173–236 [[hep-ph/9410384](#)]
- [18] J. Learned and K. Mannheim 2000 *Ann.Rev.Nucl.Part.Sci.* **50** 679–749
- [19] F. Halzen and D. Hooper 2002 *Rept.Prog.Phys.* **65** 1025–1078 [[astro-ph/0204527](#)]
- [20] J. K. Becker 2008 *Phys.Rept.* **458** 173–246 [[0710.1557](#)]
- [21] U. Katz and C. Spiering 2012 *Prog.Part.Nucl.Phys.* **67** 651–704 [[1111.0507](#)]
- [22] T. Gaisser and F. Halzen 2014 *Ann.Rev.Nucl.Part.Sci.* **64** 101–123
- [23] A. Roberts 1992 *Rev.Mod.Phys.* **64** 259–312
- [24] V. Berezhinsky and G. Zatsepin 1969 *Phys.Lett.* **B28** 423–424
- [25] K. Greisen 1966 *Phys.Rev.Lett.* **16** 748–750
- [26] G. Zatsepin and V. Kuzmin 1966 *JETP Lett.* **4** 78–80
- [27] J. Wdowczyk, W. Tkaczyk and A. W. Wolfendale 1972 *Journal of Physics A Mathematical General* **5** 1419–1432
- [28] F. Stecker 1973 *Astrophys.Space Sci.* **20** 47–57
- [29] V. Berezhinsky and A. Y. Smirnov 1975 *Astrophys.Space Sci.* **32** 461–482
- [30] M. Ahlers, L. Anchordoqui, M. Gonzalez-Garcia, F. Halzen and S. Sarkar 2010 *Astropart.Phys.* **34** 106–115 [[1005.2620](#)]
- [31] J. K. Becker 2008 *J.Phys.Conf.Ser.* **136** 022055 [[0811.0696](#)]

- [32] I. Zheleznykh 2006 *Int.J.Mod.Phys.* **A21S1** 1–11
- [33] M. A. Markov and I. M. Zheleznykh 1961 *Nuclear Physics* **27** 385 – 394 ISSN 0029-5582
- [34] J. Babson *et al.* (DUMAND Collaboration) 1990 *Phys.Rev.* **D42** 3613–3620
- [35] V. Balkanov *et al.* (BAIKAL collaboration) 2003 *Nucl.Phys.Proc.Suppl.* **118** 363–370
- [36] G. Aggouras *et al.* (NESTOR Collaboration) 2005 *Astropart.Phys.* **23** 377–392
- [37] J. Aguilar *et al.* (ANTARES Collaboration) 2006 *Astropart.Phys.* **26** 314–324
[astro-ph/0606229]
- [38] E. Migneco 2008 *J.Phys.Conf.Ser.* **136** 022048
- [39] A. Margiotta (KM3NeT) 2014 *JINST* **9** C04020 [1408.1132]
- [40] P. Bagley *et al.* 2001 *IceCube Preliminary Design Document* (The IceCube Collaboration)
<http://www.icecube.wisc.edu/science/publications/pdd/pdd.pdf>
- [41] J. Ahrens *et al.* (IceCube Collaboration) 2004 *Astropart.Phys.* **20** 507–532 [astro-ph/0305196]
- [42] M. Aartsen *et al.* (IceCube Collaboration) 2013 *Nucl.Instrum.Meth.* **A711** 73–89 [1301.5361]
- [43] F. Halzen 2013 *Riv.Nuovo Cim.* **36** 81–104
- [44] J. Beringer *et al.* (Particle Data Group) 2012 *Phys.Rev.* **D86** 010001
- [45] J. Ahrens *et al.* (AMANDA Collaboration) 2004 *Nucl.Instrum.Meth.* **A524** 169–194
[astro-ph/0407044]
- [46] M. Aartsen *et al.* (IceCube Collaboration) 2014 *JINST* **9** P03009 [1311.4767]
- [47] P. Sommers and S. Westerhoff 2009 *New J.Phys.* **11** 055004 [0802.1267]
- [48] A. M. Hillas 2006 [astro-ph/0607109]
- [49] V. Berezhinsky 2008 *J.Phys.Conf.Ser.* **120** 012001 [0801.3028]
- [50] W. Baade and F. Zwicky 1934 *Proceedings of the National Academy of Science* **20** 259–263
- [51] V. L. Ginzburg and S. I. Syrovatskii 1969 *The origin of cosmic rays*
- [52] Y. Butt 2009 *Nature* **460** 659–772 [1009.3664]
- [53] T. K. Gaisser 2001 *AIP Conf.Proc.* **558** 27–42 [astro-ph/0011524]
- [54] E. Waxman 1995 *Phys.Rev.Lett.* **75** 386–389 [astro-ph/9505082]
- [55] R. Enberg, M. H. Reno and I. Sarcevic 2008 *Phys.Rev.* **D78** 043005 [0806.0418]
- [56] M. Gonzalez-Garcia, M. Maltoni and J. Rojo 2006 *JHEP* **0610** 075 [hep-ph/0607324]
- [57] K. Daum *et al.* (Frejus Collaboration.) 1995 *Z.Phys.* **C66** 417–428
- [58] R. Abbasi *et al.* (IceCube Collaboration) 2009 *Phys.Rev.* **D79** 102005 [0902.0675]
- [59] R. Abbasi *et al.* (IceCube Collaboration) 2010 *Astropart.Phys.* **34** 48–58 [1004.2357]
- [60] R. Abbasi *et al.* (IceCube Collaboration) 2011 *Phys.Rev.* **D83** 012001 [1010.3980]
- [61] R. Abbasi *et al.* (IceCube Collaboration) 2011 *Phys.Rev.* **D84** 082001 [1104.5187]
- [62] E. Berezhko 2008 *Astrophys.J.* **684** L69–L71 [0809.0734]
- [63] T. Gaisser 1997 [astro-ph/9707283]

- [64] M. Ahlers, L. A. Anchordoqui, H. Goldberg, F. Halzen, A. Ringwald *et al.* 2005 *Phys.Rev.* **D72** 023001 [[astro-ph/0503229](#)]
- [65] TeVCat Catalog, <http://tevcat.uchicago.edu>
- [66] J. Alvarez-Muniz and F. Halzen 2002 *Astrophys.J.* **576** L33–L36 [[astro-ph/0205408](#)]
- [67] T. K. Gaisser 2013 *EPJ Web Conf.* **53** 01012
- [68] R. Abbasi *et al.* (IceCube) 2011 *Astrophys.J.* **732** 18 [[1012.2137](#)]
- [69] M. Aartsen *et al.* (IceCube Collaboration) 2013 *Phys.Rev.Lett.* **111** 021103 [[1304.5356](#)]
- [70] M. Aglietta *et al.* (LVD Collaboration) 1999 *Phys.Rev.* **D60** 112001 [[hep-ex/9906021](#)]
- [71] A. Schukraft (IceCube Collaboration) 2013 *Nucl.Phys.Proc.Suppl.* **237-238** 266–268 [[1302.0127](#)]
- [72] S. Schonert, T. K. Gaisser, E. Resconi and O. Schulz 2009 *Phys.Rev.* **D79** 043009 [[0812.4308](#)]
- [73] M. Aartsen *et al.* (IceCube Collaboration) 2014 *Phys.Rev.* **D89** 102001 [[1312.0104](#)]
- [74] P. Lipari 2006 *Nucl.Instrum.Meth.* **A567** 405–417 [[astro-ph/0605535](#)]
- [75] J. K. Becker, A. Groß, K. Münich, J. Dreyer, W. Rhode and P. L. Biermann 2007 *Astropart.Phys.* **28** 98–118 [[astro-ph/0607427](#)]
- [76] A. Silvestri and S. W. Barwick 2010 *Phys.Rev.* **D81** 023001 [[0908.4266](#)]
- [77] M. Ahlers and F. Halzen 2014 [[1406.2160](#)]
- [78] D. Wanderman and T. Piran 2010 *Mon.Not.Roy.Astron.Soc.* **406** 1944–1958 [[0912.0709](#)]
- [79] T. Glösenkamp (IceCube) 2015 [[1502.03104](#)]
- [80] B. Wang and Z. Li 2015 [[1505.04418](#)]
- [81] R. Abbasi *et al.* (IceCube Collaboration) 2012 *Nature* **484** 351–353 [[1204.4219](#)]
- [82] T. Kashti and E. Waxman 2005 *Phys.Rev.Lett.* **95** 181101 [[astro-ph/0507599](#)]
- [83] M. Gonzalez-Garcia, M. Maltoni, J. Salvado and T. Schwetz 2012 *JHEP* **1212** 123 [[1209.3023](#)]
- [84] NuFit, <http://www.nu-fit.org>
- [85] O. Mena, S. Palomares-Ruiz and A. C. Vincent 2014 *Phys.Rev.Lett.* **113** 091103 [[1404.0017](#)]
- [86] L. Fu and C. M. Ho 2014 [[1407.1090](#)]
- [87] E. Aeikens, H. PLs, S. Pakvasa and P. Sicking 2014 [[1410.0408](#)]
- [88] L. Fu, C. M. Ho and T. J. Weiler 2014 [[1411.1174](#)]
- [89] X.-J. Xu, H.-J. He and W. Rodejohann 2014 *JCAP* **1412** 039 [[1407.3736](#)]
- [90] S. Palomares-Ruiz, O. Mena and A. C. Vincent 2014 [[1411.2998](#)]
- [91] A. Palladino, G. Pagliaroli, F. Villante and F. Vissani 2015 *Phys.Rev.Lett.* **114** 171101 [[1502.02923](#)]
- [92] A. Palladino and F. Vissani 2015 [[1504.05238](#)]
- [93] L. A. Anchordoqui, H. Goldberg, F. Halzen and T. J. Weiler 2005 *Phys.Lett.* **B621** 18–21 [[hep-ph/0410003](#)]
- [94] W. Winter 2013 *Phys.Rev.* **D88** 083007 [[1307.2793](#)]
- [95] F. Halzen, A. Kappes and A. O’Murchadha 2008 *Phys.Rev.* **D78** 063004 [[0803.0314](#)]